

Role of primordial black holes in the direct collapse scenario of supermassive black hole formation at high redshifts

Kanhaiya L. Pandey^{*1} and A. Mangalam^{†1}

¹Indian Institute of Astrophysics, Bengaluru, India

Abstract

In this paper, we explore the possibility of accreting primordial black holes as the source of heating for the collapsing gas in the context of the direct collapse black hole scenario for the formation of supermassive black holes (SMBHs) at high redshifts, $z \sim 6 - 7$. One of the essential requirements for the direct collapse model to work is to maintain the temperature of the in falling gas at $\approx 10^4$ K. We show that even under the existing abundance limits, the primordial black holes of masses $\gtrsim 10^{-2} M_{\odot}$, can heat the collapsing gas to an extent that the H_2 formation is inhibited. The collapsing gas can maintain its temperature at 10^4 K till the gas reaches a critical density $n_{crit} \approx 10^3 \text{ cm}^{-3}$, at which the roto-vibrational states of H_2 approaches local thermodynamic equilibrium and H_2 cooling becomes inefficient. In the absence of H_2 cooling the temperature of the collapsing gas stays at $\approx 10^4$ K even as it collapses further. We discuss scenarios of subsequent angular momentum removal and the route to find collapse through either a supermassive star or a supermassive disk.

keywords- cosmology: theory; cosmology: dark ages, reionization, first stars; quasars: supermassive black holes.

1 Introduction

A number of bright quasars have been found at $z \gtrsim 7$ (Mortlock et al., 2011; Wu et al., 2015). These high energy sources are believed to be powered by gas accretion onto a massive ($\gtrsim 10^9 M_{\odot}$) compact region, suggesting a presence of super-massive black hole at the centre of each of these quasars. The existence of such SMBHs with masses $\approx 10^9 M_{\odot}$ at the time when the Universe had just spent $\approx 5\text{-}6\%$ (≈ 700 Myr) of its total age, raises a big question of how such massive black holes could have been formed so early in the Universe. There are three main proposals in the literature for black hole genesis, all of which have caveats. The first one starts with star clusters, which if compact enough, can suffer runaway collisions that could lead to a single collapsed star with a mass of about $100 M_{\odot}$. Simulations of this scenario suggest that black hole seed formation is not sufficiently efficient; besides this, it is not clear how these dense star clusters are formed in the first place (Volonteri & Bellovary, 2012).

Another idea is that seed black holes are formed from single massive stars; in case of Pop I and II stars, the presence of metals enhances opacity and limits the mass of the star that collapses to black holes due to excessive stellar winds and mass loss. So, it is the first generation of stars (the Pop III stars) that would leave behind black holes of masses of at least $\approx 100 M_{\odot}$, early enough by the redshifts as high as $z \sim 20 - 25$ (Abel et al., 2002; Bromm et al., 2002; O’Shea & Norman, 2007). However, growing these seed black holes by gas accretion at Eddington rate would take $\approx 10^8$ years to reach a mass of around $10^9 M_{\odot}$ (Salpeter, 1964), which is much longer than the time available to reach it by $z \sim 7$. Although, one can assume a sufficiently efficient gas accretion to make it work, but it turns out that the accretion has to be highly super-Eddington (Smole et al., 2015). Such efficient growth by accretion is very unlikely due to many feedback effects such

^{*}kanhaiya.pandey@iiap.res.in

[†]mangalam@iiap.res.in

as radiation pressure and photoionization heating, which can lead to a severe disruption of the accretion flow. Also, neighboring Pop III stars in the vicinity of the seed black hole, and the seed black hole itself may ionize the surrounding gas causing suppression of subsequent accretion onto the progenitor seed black hole [Safraneck-Shrader et al. \(2012\)](#). Merging of the black holes can also play an essential role in the formation of the SMBHs, but it turns out to be difficult as well, typically the number of mergers required is too high. Very frequent halo mergers would result in the formation of small N-body systems of BH seeds, which would be prone to SMBH slingshot ejections from the DM halo ([Haiman, 2004](#); [Volonteri, 2007](#)).

An appealing alternative class of models called the direct collapse black hole (DCBH) model for the formation of SMBHs involves formation of a SMBH seed of mass $\sim 10^5 M_\odot$, by the redshift of $z \sim 10 - 20$ through a rapid collapse of primordial (metal-free) gas in a high density, high inflow rate environment in which star formation is suppressed ([Oh & Haiman, 2002](#); [Bromm & Loeb, 2003](#); [Volonteri & Rees, 2005](#); [Begelman et al., 2006](#)). This model has gained an increasing interest following a recent observation of highly luminous Ly α emitter galaxy (CR7) at $z \sim 6.6$. The observational features of the galaxy CR7 (such as absence of metal lines, presence of Ly α and He II 1640 Å line with a large +160 km/s offset) put together fits very well with the DCBH modeling of the data, indicating that the object CR7 contains a direct collapse black hole in making at its centre ([Smith et al., 2016](#)).

In the context of DCBH formation model, the issues anticipated in the case of Pop III seed scenario do not play any important role. In order to make this model work, the collapsing gas must avoid fragmentation, shed angular momentum efficiently, and collapse rapidly. For these conditions to be met, the gas needs to keep its temperature high enough ($\sim 10^4$ K). This kind of rapid gas collapse can be expected in relatively massive dark matter halos with virial temperature $T_{vir} \gtrsim 10^4$ K. However, recent numerical simulations ([Shang et al., 2010](#)) find that the collapsing gas in such halos forms H₂ efficiently and cools to temperatures $\lesssim 300$ K.

The H₂ cooling is an important concern in the DCBH scenario. However, if the in falling gas is exposed to an intense Lyman-Werner (band near photon energy ~ 12 eV) UV flux coming from sources in its vicinity, the formation of H₂ can be suppressed (either by directly photo-dissociating H₂ or by photo-dissociating intermediary H⁻) and thus the H₂ cooling can be avoided. The critical LW flux needed for this to happen is much higher, $J_{crit}^{LW} \gtrsim 10^{2-5}$, ([Shang et al., 2010](#); [Omukai, 2001](#); [Bromm & Loeb, 2003](#)) than the expected level of cosmic UV background at those high redshifts, eg. $J^{LW} \sim 1$ at $z \sim 10$ ([Trenti & Stiavelli, 2009](#))¹. However, the flux seen by an individual halo may fluctuate by many orders of magnitude depending on the distance of the source from the halo, a possible high enough LW flux coming from nearby source can potentially contaminate the collapsing halo with metals and thus making the collapsing gas cool much faster and consequently fragment.

A lot of scenarios have been studied to circumvent the H₂ cooling in the context of SMBH formation models, such as [Sethi et al. \(2010\)](#) and the references therein. We explore the possibility of accreting primordial black holes as the heating source. The idea that primordial black holes (PBHs) might comprise some or all of the dark matter has been around for many decades. Also this hypothesis has been tested by various observations such as, extragalactic γ -ray background, OGLE (The Optical Gravitational Lensing Experiments)-I,II (MACHO and EROS), III & IV, microlensing from Kepler, Eridanus-II star cluster, and CMB experiments such as WMAP and Planck ([Carr et al. \(2016\)](#) and references therein, [Ricotti et al. \(2008\)](#); [Clark et al. \(2017\)](#)), which gave rise to strong bounds on PBH abundances in various mass windows. Even with the latest experiments there are certain mass ranges for which f_{PBH} ($= \Omega_{PBH}/\Omega_m$) could be as high as 10%.

We use the following form of the Ω_{PBH} for our calculation. This particular form is a simpler adaptation of the constraints on the PBH abundances in the mass range of the interest ($10^{-4}M_\odot - 10^4M_\odot$), see [Figure 1](#).

$$\Omega_{PBH} = \begin{cases} 25 \times \left(\frac{m_{PBH}}{M_\odot}\right)^{-2} \Omega_m, & m_{PBH} > 25 M_\odot \\ 0.04 \Omega_m, & m_{PBH} < 25 M_\odot \end{cases} \quad (1)$$

where m_{PBH} is the mass of the individual PBH, Ω_m is the cosmological dark matter density parameter.

We assume that a portion (f_{PBH}) of dark-matter is made up of primordial black holes of a certain mass, which are uniformly distributed inside the dark matter halo. We discuss some findings on the possible

¹ J^{LW} is in units of $10^{-21} \text{ erg s}^{-1} \text{ Hz}^{-1} \text{ str}^{-1} \text{ cm}^{-2}$.

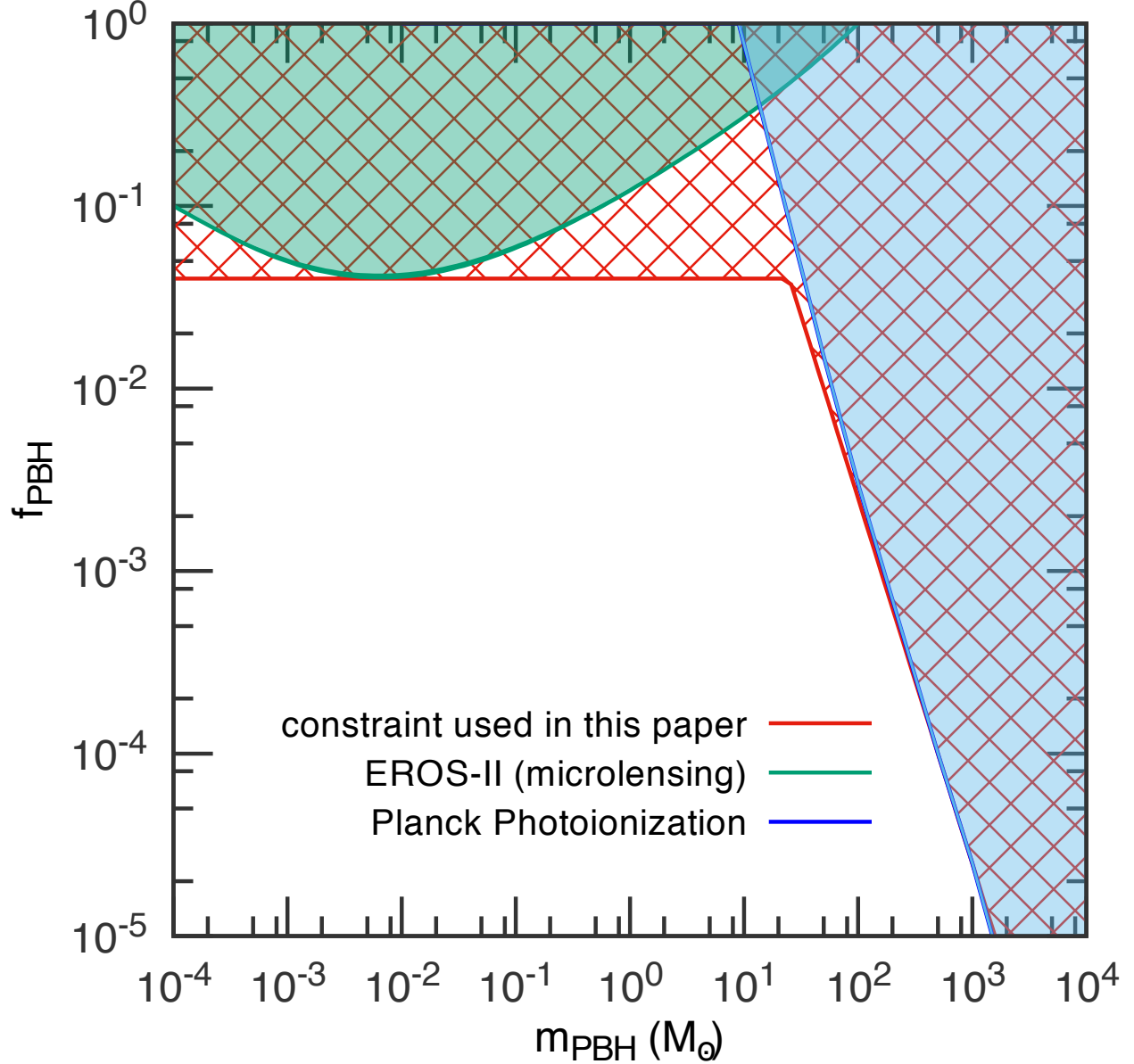


Figure 1: Constraints on $f_{PBH} = \Omega_{PBH}/\Omega_m$ coming from micro-lensing from EROS-II (Carr et al., 2017, monochromatic constraints), Planck (Ali-Haïmoud & Kamionkowski, 2017, assuming photoionization through PBH accretion) and the constraint which we have used in this paper, are shown above.

cosmological evolution of primordial black holes (Rice & Zhang, 2017) using a detailed Eddington limited cosmic accretion history of all components of baryons, dark matter (WIMPs) and radiation:

- PBHs with a wide range of masses could have been formed in the very early Universe as a result of the direct collapse of large over-densities (Hawking, 1971; Clark et al., 2017).
- A PBH with mass $< 10^{14}$ g will not accrete radiation or matter at a rapid enough rate and will evaporate due to Hawking radiation.
- A PBH with initial mass (in g) in the range $10^{15} < M_{PBH} < 10^{28}$ neither evaporates or accretes significantly over Hubble time.

- A PBH with initial mass (in g) in the range $10^{28} < M_{PBH} < 10^{29}$ accretes significantly during the era after recombination and before thermalization of baryons with radiation, $z_{th} \sim 174 < z < z_{rec} \simeq 1100$ at Eddington limited Bondi rates. The mass changes by an order of magnitude over this time and subsequently increases only by a small fraction.
- It is unlikely for PBHs to grow to large black holes by $z \sim 6$ by Eddington limited accretion.

With this in mind, we now turn our attention to the extent to which the radiation from these accreting PBH can heat the ambient Universe in the from post-recombination era to $z \sim 7$.

The f_{PBH} is a function of the mass of the PBH (m_{PBH}) and is taken from the most recent constraints on the PBH abundance. We use a monochromatic abundance limit on PBH of masses around $1 M_{\odot}$, as suggested by [Ali-Haïmoud & Kamionkowski \(2017\)](#). These limits are for accreting primordial black holes using the recent Planck CMB temperature and polarization data. They have considered the effect of the radiation coming from the PBH accretion on the collisional ionization and the photoionization in the ambient medium. The constraints coming from the photoionization considerations are stronger, and to be conservative we have taken the stronger constraint on f_{PBH} quoted by them. For masses below $1 M_{\odot}$ we use the EROS-II microlensing constraints ([Tisserand et al., 2007](#)). We find that even under the given constraints on the PBH abundances [though we use a little stronger constraints to be more conservative, Equation (1), Figure 1], accreting PBHs of masses $\gtrsim 10^{-2} M_{\odot}$, uniformly distributed in a dark matter halo, can provide enough heating for the collapsing gas to suppress the H_2 formation and hence the gas can avoid the H_2 cooling.

We would like to emphasize here that, unlike the case of the suppression of H_2 abundance through LW flux, where the H_2 molecules are directly gets destroyed by the radiation, in this scenario, the suppression of H_2 abundance is due to the suppression in the H_2 formation rate because of higher temperature of the gas. Also in this scenario, there is no issue of contamination of the gas with heavy metal coming from nearby LW sources (stars).

2 Thermodynamical evolution in DCBH scenario with accreting PBH heating

We carry out a study of a collapsing gas into the potential well of dark matter halo of mass $M_h = 10^8 M_{\odot}$. The initial condition is set to be as $\delta_i = 0.04$ at $z = 1000$, (a 6-7 σ fluctuation with the collapse redshift $z_{col} \sim 25$). Initially, the gas traces the evolution of the dark matter till the dark matter gets virialized and turns into a dynamically stable halo. After dark matter virialization, gas collapses into the gravitational potential of the dark matter halo as it loses its pressure support through various cooling processes. For the thermal evolution of the collapsing gas, we use the prescription given in the [Clark et al. \(2017\)](#), with an additional term in heating given by accreting primordial black holes ($dE_{PBH}/dVdt$), and we also include atomic H and molecular H_2 cooling (Equation 25). For H and H_2 cooling we follow the prescription given in [Sethi et al. \(2010\)](#).

2.1 Dynamical evolution of the collapsing gas

We use the simple spherical top-hat model for the collapse of the matter till the dark matter halo reaches virialization. We assume that till this stage the dark matter and the baryons follow each other. The evolution of the radius of the encompassing shell in comoving coordinates is computed using the following equations:

$$r(z) = r_i \frac{1 + \delta_i}{2\delta_i} (1 - \cos \eta(z)) \quad (2)$$

$$\frac{t(z)}{t_i} = \frac{\eta(z) - \sin \eta(z)}{\eta_i - \sin \eta_i} \quad (3)$$

where $\cos \eta_i \equiv 1 - 2\delta_i/(1 + \delta_i)$ and

$$r_i = \left(\frac{3M_i}{4\pi(1 + \delta_i)\rho_i^{crit}} \right)^{1/3} \quad (4)$$

$$\rho_i^{crit} = \frac{3H_0 E(z_i)}{8\pi G} \quad (5)$$

$$t(z) = \frac{1}{H_0} \int_z^\infty \frac{dz}{(1+z)E(z)} \quad (6)$$

where $E(z) = (\Omega_m(1+z)^3 + \Omega_\Lambda)^{1/2}$ and $M_i = M_h(\Omega_m/\Omega_c)$. Ω_m , Ω_c and Ω_b are respectively density parameter for the total matter, dark matter and baryons ($\Omega_m = \Omega_c + \Omega_b$). Since at high redshifts, the Universe was matter dominated, we can safely use the above mentioned spherical top hat equations for the dynamical evolution of the dark matter halo. The gas is assumed to follow the dark matter halo till virialization. After virialization, the baryonic gas falls into the virialized dark matter halo by losing its thermal energy due to inverse-Compton, atomic H, and molecular H₂ cooling. We evolve gas density after dark matter virialization until it reaches a number density of \approx a few 1000 per cc, using simple a gravitational collapse given by

$$\frac{d^2 r}{dt^2} = -\frac{GM(r)}{r^2} \quad (7)$$

$$M(r) = M_h \left(\frac{\Omega_b}{\Omega_c} + \left(\frac{r}{R_v} \right)^3 \right) \quad (8)$$

where $R_v = r_i(1 + \delta_i)/(2\delta_i)$ is the virial radius for the dark matter halo. Here, r is co-moving radius of the baryon sphere that by definition contains all the baryons of mass ($M_b = M_h\Omega_b/\Omega_c$) and the contribution to $M(r)$ due to the uniformly distributed dark matter $(r/R_v)^3 M_h$ decreases.

2.2 Heating due to primordial black holes

The rate of accretion of mass onto an individual PBH is taken as the minimum of the Bondi accretion rate and the Eddington accretion rate,

$$\dot{m}_{\text{PBH}} = \min \left(\frac{\pi G \rho_b}{c_s^3} \dot{m}_{\text{PBH}}^2, \frac{4\pi G m_p}{\sigma_T c} \dot{m}_{\text{PBH}} \right) \quad (9)$$

where G is the gravitational constant, ρ_b is infalling gas density and c_s is the sound speed in the infalling gas, σ_T is Thompson scattering cross-section, c is speed of light and the m_p is the mass of proton.

The total energy produced per unit comoving volume per unit time by the accretion of mass onto primordial black holes can be given by,

$$\frac{dE_{\text{PBH}}}{dV dt} = \dot{E} \left(\frac{\#PBH}{Volume} \right) = \epsilon \frac{\dot{m}_{\text{PBH}}}{m_{\text{PBH}}} c^2 \Omega_{\text{PBH}} \rho_{c0} (1+z)^3 \quad (10)$$

where ρ_{c0} is the critical density of the Universe today and z is the redshift.

Accretion theory is replete with various possible scenarios of accretion; the most apt mode for PBH could be advection dominated disk accretion flow [ADAF, [Narayan & Yi \(1995\)](#)] or sub-Eddington Bondi accretion ([Bondi, 1952](#)) beside the usual thin disk mode ([Shakura & Sunyaev, 1973](#)). Based on relativistic theory it is reasonable to assume an accretion efficiency of $\epsilon = 1 - \sqrt{1 - 2/(3r_I)} = 0.06 - 0.43 \sim 0.1$ where r_I is the ISCO radius that varies from $6 \rightarrow 1$ as the spin varies from $a = 0 \rightarrow 1$. However, the detailed geometry and the accretion mode play a key role in determining ϵ . For example, in case of thin disks it has been seen from observations and theoretical models that $\epsilon \sim 0.1$ for $\dot{m}_{\text{PBH}} > \dot{m}_E$ ([Park & Ostriker, 2001](#)). The sub-Eddington flows are known to be radiatively inefficient ([Heinz & Sunyaev, 2003](#)). If the accretion is sub-Eddington, $\dot{m}_{\text{PBH}} < \dot{m}_E$, then the radiative efficiency $\epsilon \propto \dot{m}_{\text{PBH}}$. A conservative estimate considering various allowed modes for PBH accretion has been suggested to take a simple form ([Ricotti et al., 2008](#)); we

take it to be $< 10\%$ and assume it to be $\propto \dot{m}$. For the maximum radiative efficiency we have taken a typical value as 10% . To summarize our assumption,

$$\epsilon = \begin{cases} 0.1, & \frac{\dot{m}_{\text{PBH}}}{\dot{m}_{\text{E}}} \geq 1 \\ 0.1 \frac{\dot{m}_{\text{PBH}}}{\dot{m}_{\text{E}}}, & \frac{\dot{m}_{\text{PBH}}}{\dot{m}_{\text{E}}} < 1 \end{cases} \quad (11)$$

where \dot{m}_{E} is the Eddington rate.

2.3 Thermal evolution of the collapsing gas

Our prescription for the thermal evolution of the collapsing gas is based on the prescription given in [Clark et al. \(2017\)](#). We have added an additional term for the accreting primordial black hole heating and we also incorporate cooling (Equation 25). The evolution of the gas temperature (T_g), ionization fraction (x_e) and H_2 fraction (x_{H_2}) is calculated by solving coupled differential Equations (12–14):

$$\frac{dT_g}{dt} = -2 \frac{v_r}{r} T_g + \left(\frac{m_p}{m_e} \frac{2\alpha_t}{(1+x_e)} + \frac{x_e^2 \Gamma_B}{1+x_e} \right) (T_\gamma - T_g) - \frac{2K_h}{3k_B(1+f_{\text{He}}+x_e)} \quad (12)$$

$$\frac{dx_e}{dt} = \left[\beta_e(1-x_e) e^{\left(\frac{-E_\alpha}{k_B T_\gamma}\right)} - x_e^2 \alpha_e n_b - (I_{\chi\alpha} + I_{\chi i}) \right] C \quad (13)$$

$$\frac{dx_{\text{H}_2}}{dt} = k_{\text{form}} n_b x_e (1-x_e-2x_{\text{H}_2}) - k_{\text{des}} n_b x_{\text{H}_2} \quad (14)$$

Here r is the comoving radius of the outer most shell of the gas and v_r is its radial velocity, T_γ is the CMB temperature which evolves as $T_\gamma(z) = 2.725(1+z)$ and $n_b = \rho_b/m_p$ is the baryon number density of the infalling gas.

The Compton friction α_t is given by,

$$\alpha_t = \frac{4}{3} \frac{\epsilon_\gamma \sigma_T x_e}{m_p c} \quad (15)$$

where ϵ_γ is the radiation energy density (aT_γ^4 , a is radiation constant). The effective recombination rate and the photoionization rate, α_e and the β_e respectively, are given by,

$$\alpha_e = 2.84 \times 10^{-13} \left(\frac{T_\gamma}{10^4 \text{ K}} \right)^{-1/2} \quad (16)$$

$$\beta_e = \alpha_e \exp\left(-\frac{E_2}{k_B T_\gamma}\right) \left(\frac{\sqrt{2\pi k_B m_e T_\gamma}}{h_p} \right)^3 \quad (17)$$

where E_2 is the energy of the Hydrogen atom at $n=2$ level, k_B is the Boltzmann constant, h_p is the Planck's constant and m_e is the mass of an electron. The C factor in the Equation (13) is given by

$$C = \frac{1 + K n_{\text{H}} \Lambda_{21} (1-x_e)}{1 + K (\beta_e + \Lambda_{21}) n_{\text{H}} (1-x_e)} \quad (18)$$

where n_{H} is hydrogen number density, Λ_{21} ($=8.23$) is the decay rate for the transition between the levels 2s to 1s of the hydrogen atom and the parameter K is given by,

$$K = \frac{\lambda_\alpha^3}{8\pi H} \quad (19)$$

where λ_α is the wavelength of the Ly- α transition and E_α is the energy corresponding λ_α , and H is the Hubble parameter.

Γ_B is the temperature equilibration time due to Bremsstrahlung absorption and emission given by,

$$\Gamma_B^{-1} = 4.6 \times 10^9 \left(\frac{T_g}{10^3 \text{ K}} \right)^{1/2} \left(\frac{g_B n_{\text{H}}}{10^3 \text{ cm}^{-3}} \right)^{-1} \quad (20)$$

where $g_B \approx 1.2$ is the averaged Gaunt factor.

The quantities $I_{\chi\alpha}$, $I_{\chi i}$, and K_h are factors corresponding to the additional energy injection (in our case the PBH heating) which affects the ionization from the ground state, ionization from excited states, and heating of the collapsing gas. The quantity $I_{\chi\alpha}$ is the ionization rate of hydrogen atom from $n=2$ due to PBH heating, $I_{\chi i}$ is the direct ionization rate of the hydrogen atom, K_h is the fraction of the total energy injection going in to the heating of the medium. Each of these injections is dependent on the injection energy through:

$$I_{\chi\alpha} = \frac{(1 - C) (dE/dVdt) \chi_\alpha}{E_\alpha n_H} \quad (21)$$

$$I_{\chi i} = \frac{(dE/dVdt) \chi_i}{E_i n_H} \quad (22)$$

$$K_h = \frac{(dE/dVdt) \chi_h}{n_H} \quad (23)$$

Here n_H is the hydrogen number density, and E_i is the ionization energy for the ground state electron in hydrogen atom and E_α is the difference in binding energy between the $n=1$ and the $n=2$ electron energy levels. The quantity C is related to the probability for an excited hydrogen atom to emit a photon prior to being ionized (Clark et al., 2017). The quantities χ_α , χ_i and χ_h are efficiencies for energy interactions through each channel, and are taken to be in the following form (Madhavacheril et al., 2014)

$$\chi_\alpha = \chi_i; \quad \chi_i = \frac{1}{3}(1 - x_H); \quad \chi_h = \frac{1 + 2x_H + f_{He}(2x_{He} + 1)}{3(f_{He} + 1)} \quad (24)$$

where x_H is the ratio of ionized hydrogen to total hydrogen, x_{He} is the ratio of ionized helium to total helium and f_{He} is the helium fraction given by $f_{He} = Y_p/(4(1 - Y_p))$ where Y_p is the helium mass fraction ($= 0.24$). In reality, the fraction of energy going in to ionization of the ambient medium is more complex than the simple linear form given by the Equation (24), however we use this equation as it as a good approximation (Madhavacheril et al., 2014).

The total effective energy injection rate per volume is given by

$$\frac{dE}{dVdt} = \frac{dE_{PBH}}{dVdt} - L_{cool} \quad (25)$$

where $dE_{PBH}/dVdt$ is the heating due to accreting primordial black holes and the L_{cool} is the cooling due to the atomic and molecular hydrogen cooling.

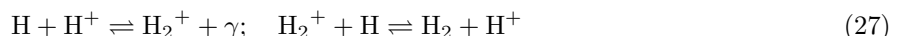
2.4 Atomic (H) and molecular hydrogen (H₂) cooling

Since the collapsing gas is metal free the only dominant cooling mechanism apart from the atomic hydrogen line cooling and the inverse-Compton process is the molecular hydrogen (H₂) cooling. The atomic hydrogen cooling is dominant when the temperature of the gas is $\gtrsim 10^4$ K, below this temperature the H I line cooling becomes inefficient and H₂ cooling takes over.

To compute the atomic and molecular hydrogen cooling functions (L_{cool}) we follow the prescription given in Hollenbach & McKee (1979) and Galli & Palla (1998).

2.5 Evolution of molecular hydrogen (H₂) fraction

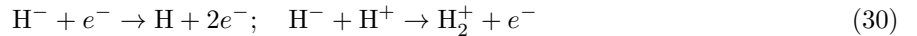
In the set up of the high redshift Universe (metal-free gas) the following reactions are the important channels for the formation and destruction of H₂ molecules (Sethi et al., 2010, 2008),



Reaction	Reaction rate coefficient k ($\text{cm}^3 \text{s}^{-1}$)
$\text{H} + e^- \rightarrow \text{H}^+ + 2e^-$	$k_1 = 3 \times 10^{-16} (T_\gamma/300)^{0.95} \exp(-T_\gamma/9320)$
$\text{H} + e^- \rightarrow \text{H}^- + \gamma$	$k_9 = 6.775 \times 10^{-15} T_{eV}^{0.8779}$
$\text{H}^- + \text{H} \rightarrow \text{H}_2 + e^-$	$k_{10} = 1.43 \times 10^{-9}$ for $T_{eV} \leq 0.1$ $k_{10} = \exp\{-20.069 + 0.229(\ln T_{eV}) + 0.036(\ln T_{eV})^2\}$ for $T_{eV} > 0.1$
$\text{H}^- + \text{H}^+ \rightarrow 2\text{H}$	$k_{13} = 6.5 \times 10^{-9} T_{eV}^{-0.5}$
$\text{H}_2 + \text{H} \rightarrow 3\text{H}$	$k_{15} = 5.24 \times 10^{-7} T^{-0.485} e^{-52000/T}$
$\text{H}_2 + \text{H}^+ \rightarrow \text{H}_2^+ + \text{H}$	$k_{17} = \exp\{-24.249 + 3.401(\ln T_{eV}) - 3.898(\ln T_{eV})^2\}$
$\text{H}_2 + e^- \rightarrow 2\text{H} + e^-$	$k_{18} = 5.6 \times 10^{-11} e^{-102124/T} T^{0.5}$
$\text{H}^- + e^- \rightarrow \text{H} + 2e^-$	$k_{19} = \exp\{-18.018 + 2.361(\ln T_{eV}) - 0.283(\ln T_{eV})^2\}$
$\text{H}^- + \text{H} \rightarrow 2\text{H} + e^-$	$k_{20} = 2.56 \times 10^{-9} \times T_{eV}^{1.78186}$ for $T_{eV} \leq 0.1$ $k_{20} = \exp\{-20.373 + 1.139(\ln T_{eV}) - 0.283(\ln T_{eV})^2\}$ for $T_{eV} > 0.1$
$\text{H}^- + \text{H}^+ \rightarrow \text{H}_2^+ + e^-$	$k_{21} = 4.0 \times 10^{-4} \times T^{-1.4} \times e^{-15100/T}$ for $T \leq 10^4$ $k_{21} = 10^{-8} T^{-0.4}$ for $T > 10^4$
$\text{H}^- + \gamma \rightarrow \text{H} + e^-$	$k_\gamma = 4 \left(\frac{2\pi m_e k_B T_\gamma}{h^2} \right)^{3/2} \exp\left(\frac{-0.754eV}{k_B T_\gamma} \right) k_1$

Table 1: Reaction rates coefficients (Shang et al., 2010; Bovino et al., 2014; Sethi et al., 2008). In the table $T \equiv T_g$ and T_{eV} is T_g in units of electron-Volts.

Also, the destruction of H_2 can be due to the destruction of intermediary H^- through following reactions,



For the H_2 formation and destruction rates, we follow Sethi et al. (2010) and the references therein. The net rate of formation, k_{form} , and destruction, (k_{des}) of H_2 is taken as

$$k_{form} = \frac{k_9 k_{10} x_{\text{H}^-} n_b}{k_{10} x_{\text{H}^-} n_b + k_\gamma + (k_{13} + k_{21}) x_p n_b + k_{19} x_e n_b + k_{20} x_{\text{H}^-} n_b} \quad (31)$$

$$k_{des} = k_{15} x_{\text{H}^-} + k_{17} x_p + k_{18} x_e \quad (32)$$

For all the above reaction rates, we follow the Shang et al. (2010) and Sethi et al. (2008) except for k_{15} which is a three-body reaction ($\text{H}_2 + \text{H} \rightleftharpoons 3\text{H}$) rate, for which we follow recent results from Bovino et al. (2014). A list of all these reaction rates is given in the Table 1, which only shows the leading terms; for the actual fit, please see the references.

3 Effect of PBH heating

The Figures 2-4 show the evolution of the temperature, T_g , the ionization fraction, x_e , and the H_2 fraction, x_{H_2} . The time evolution in these figures is towards the right. The gas density falls (as the halo expands with

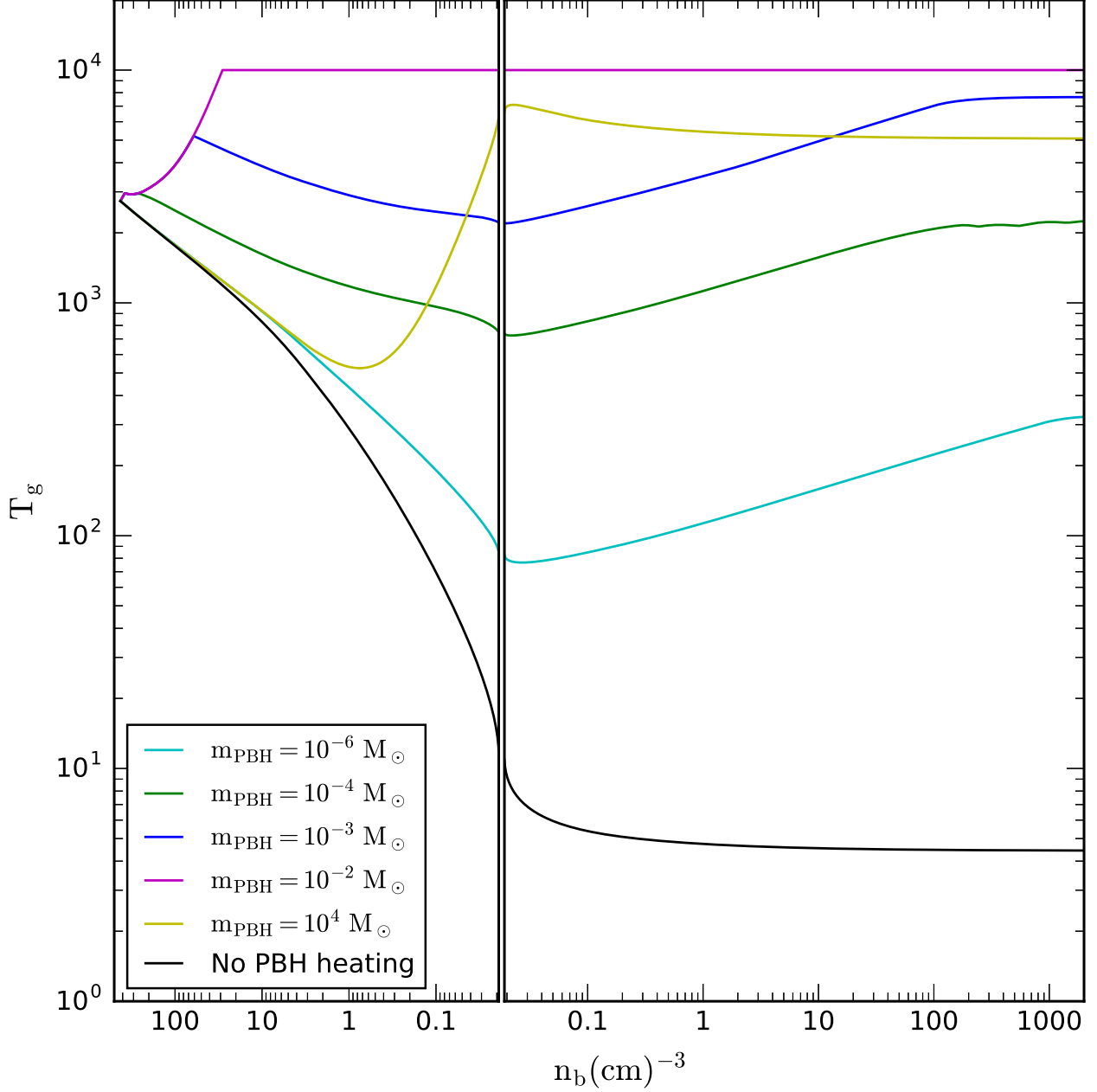


Figure 2: The evolution of gas temperature T_g with gas density n_b as it collapses is shown for various values of the PBH mass m_{PBH} . The left panel shows the expansion phase whereas the right panel shows the collapse phase.

the background Universe) until the turnaround, and then increases again as the halo collapses. The figures show the interplay between several physical effects. The accretion rate for a higher mass PBH is more and therefore the heating also increases with the mass of the PBHs. The PBH heating increases the temperature of the gas which increases the ionization fraction due to enhanced collisional ionization. However, the increase in temperature play a complicated role in the evolution x_{H_2} ; it increases the collisional destruction rate of H_2 but at the same time an increase in ionization fraction, x_e , tends to increase the formation rate of H_2 competing with its collisional dissociation. H_2 cooling depends on the temperature as well as the molecular hydrogen fraction.

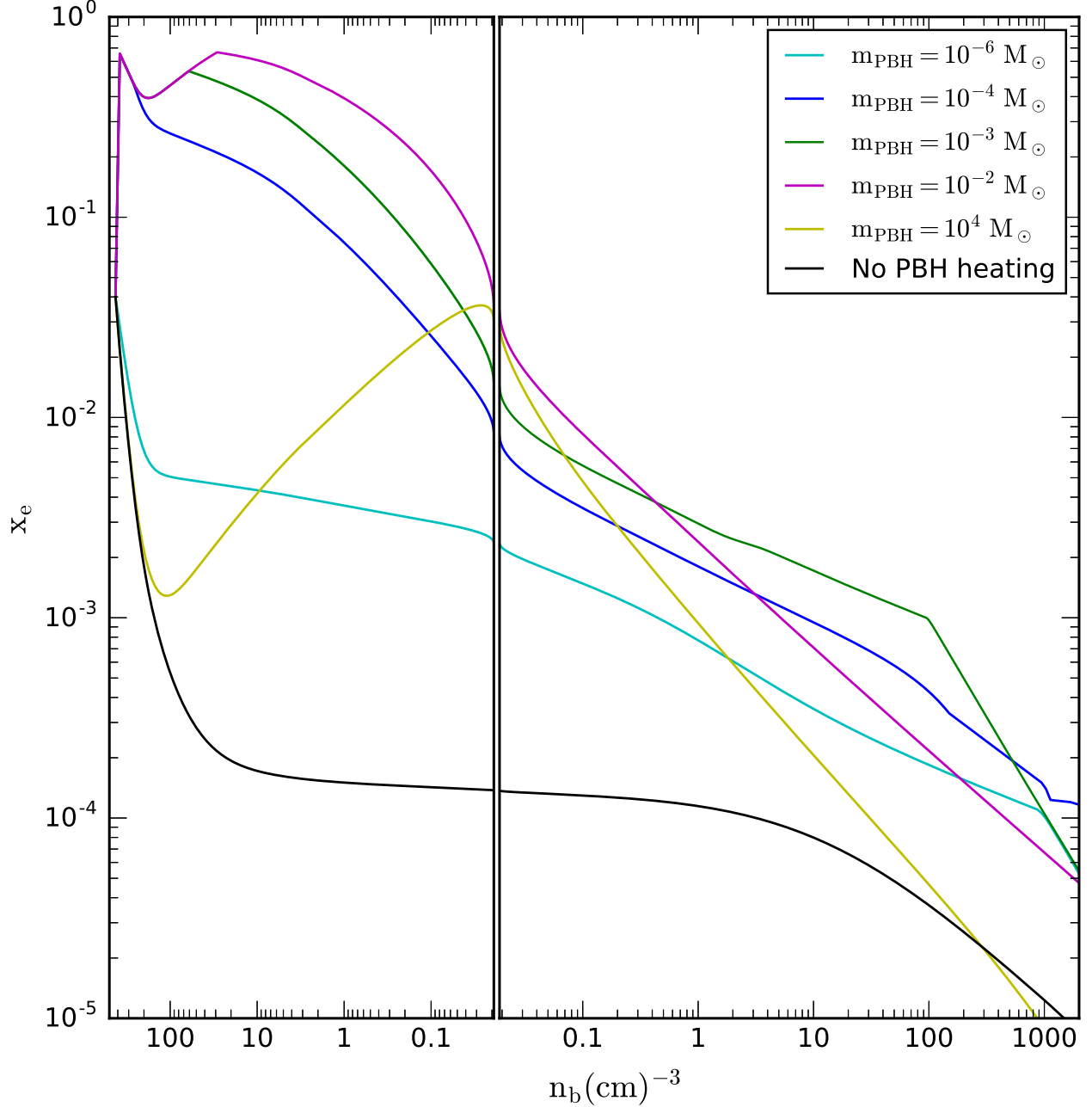


Figure 3: The evolution of ionization fraction x_e with gas density n_b as it collapses is shown for various values of the PBH mass m_{PBH} . The left panel shows the expansion phase whereas the right panel shows the collapse phase.

Figures 5-6 show the relative strength of various heating and cooling mechanisms involved for the case of $m_{\text{PBH}} = 10^{-6} M_\odot$ and $m_{\text{PBH}} = 10^{-2} M_\odot$ respectively. We can clearly see from these figures that for lower mass ($10^{-6} M_\odot$) PBH heating, H_2 -cooling eventually wins, whereas in the case of sufficiently higher mass ($10^{-2} M_\odot$) PBH heating is high enough to be able to suppress the H_2 cooling. In this case, the temperature of the collapsing gas can rise until it reaches 10^4 K, beyond which the HI line cooling takes over, which is an efficient cooling process for the collapsing gas which is optically thin, and therefore the temperature of the collapsing gas does not rise above the 10^4 K.

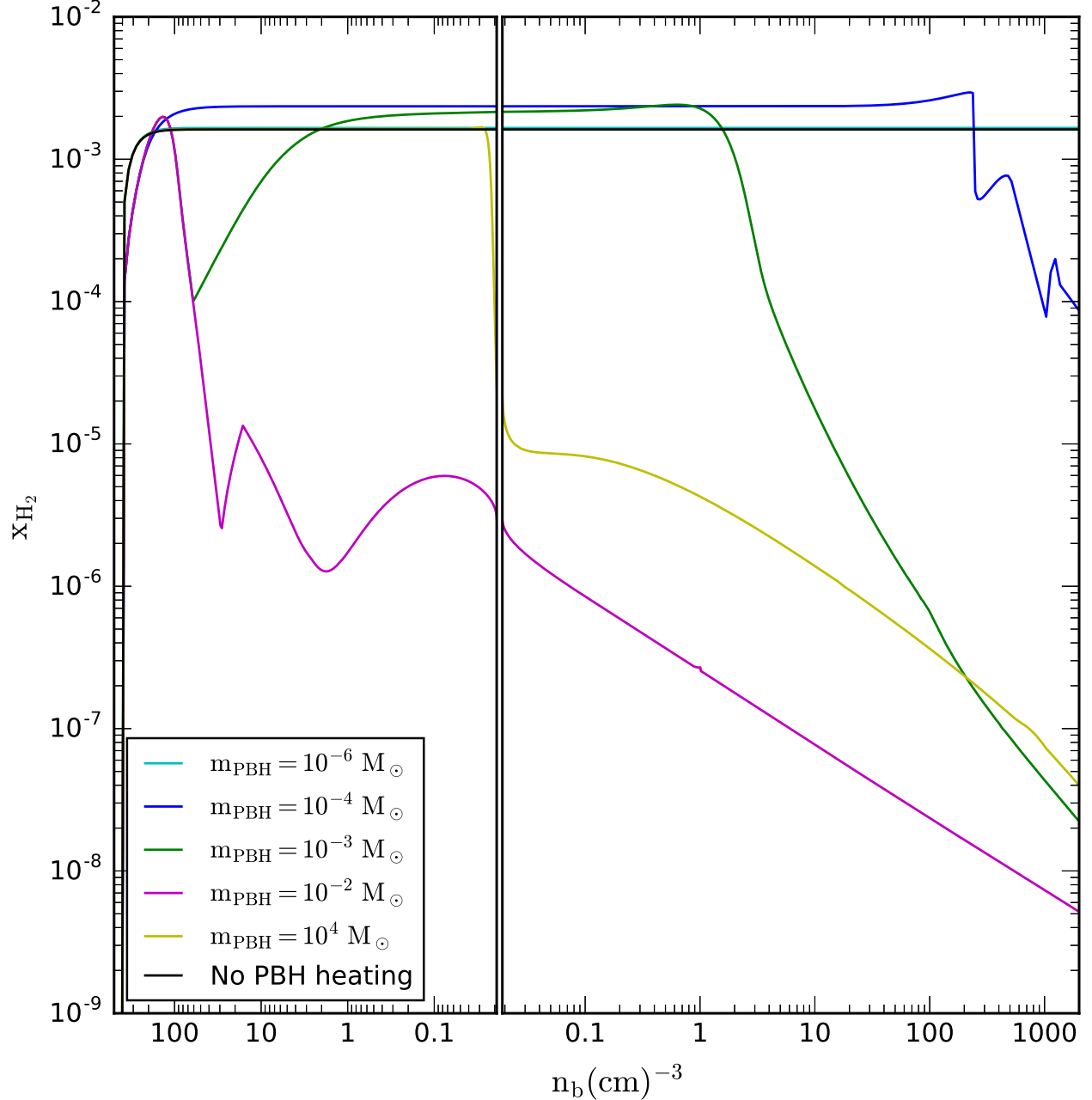


Figure 4: The evolution of H_2 fraction x_{H_2} with gas density n_b as it collapses is shown for various values of the PBH mass, m_{PBH} . The left panel shows the expansion phase whereas the right panel shows the collapse phase.

With the low mass PBH heating, the H_2 formation increases very rapidly and results in a lowering of temperature due to H_2 cooling which in turn drop the ionization fraction. But for high enough heating rate H_2 dissociation finally takes over and the H_2 fraction drops rapidly in the collapsing phase of the gas; thus the H_2 cooling become weak. At the same time, as the halo gas collapses further, in the high density environment aided with the high temperature, the three body destruction rate of H_2 becomes important and the H_2 fraction goes down even more rapidly. Once a critical density reaches a value $n_b \gtrsim 1000$ per cc, the roto-vibrational states of H_2 molecules reaches a local thermodynamic equilibrium and H_2 cooling becomes

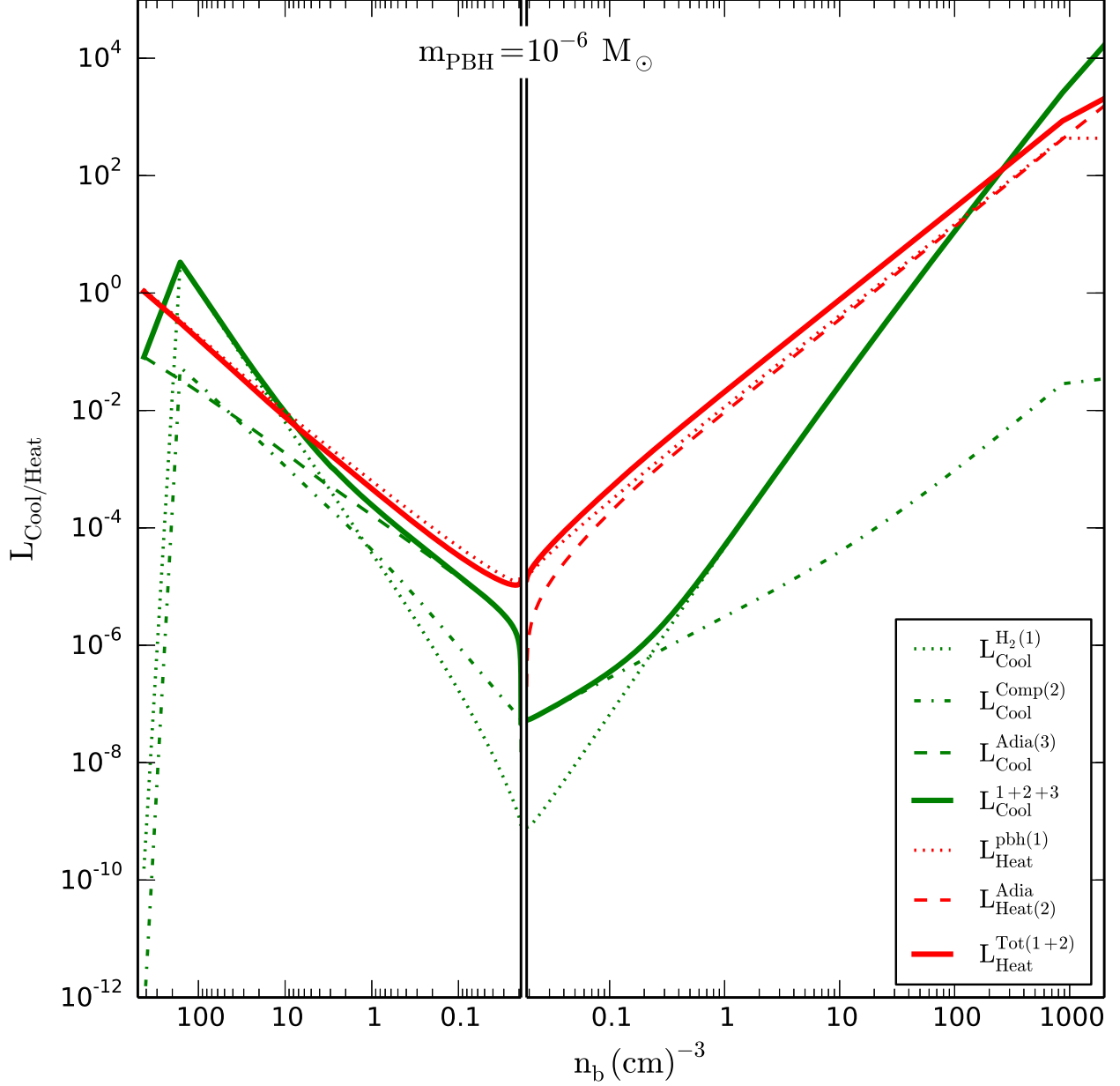


Figure 5: Relative strengths of various heating and cooling processes involved (H_2 -cooling, Compton cooling, adiabatic cooling/heating, PBH heating), for the case of $m_{\text{PBH}} = 10^{-6} M_{\odot}$. The rates are in the units of $\sim H_0 dt/dz = \Omega_m^{-1/2} (1+z)^{-5/2}$.

inefficient. Therefore the further gas collapse is not affected by the H_2 cooling and the temperature of the gas remains near $\sim 10^4$ K.

We carried out the calculation for higher values of PBH masses and found that for any value of PBH mass above $\sim 10^{-2} M_{\odot}$ it is possible to heat the collapsing gas enough to avoid the H_2 cooling. Though for very high mass ($\gtrsim 10^4 M_{\odot}$) PBHs the allowed abundance limit is too low to produce enough heating (see Figure 2).

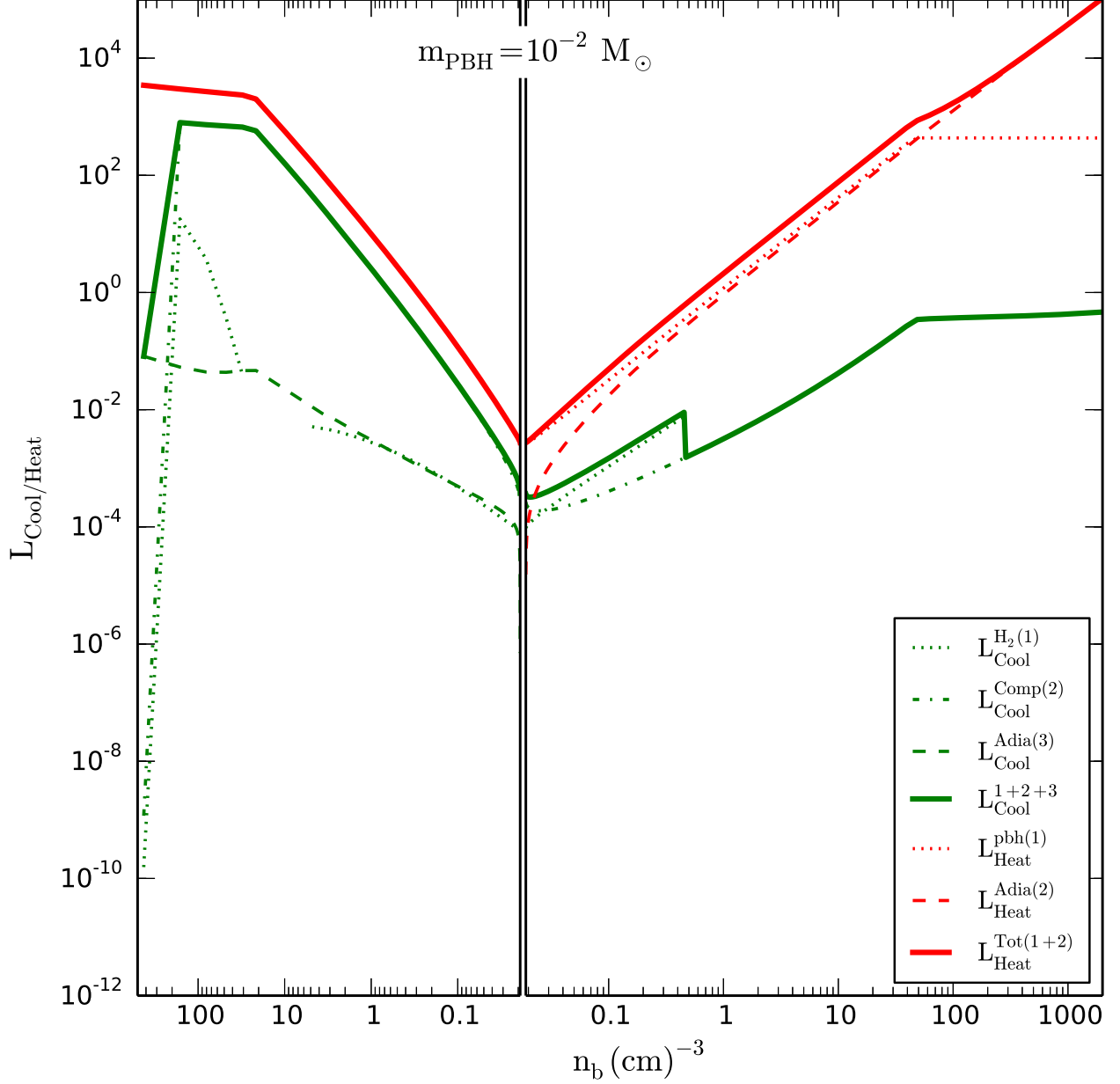


Figure 6: Relative strengths of various heating and cooling processes involved (H₂-cooling, Compton cooling, adiabatic cooling/heating, PBH heating), for the case of $m_{\text{PBH}} = 10^{-2} M_{\odot}$. The rates are in the units of $\sim H_0 dt/dz = \Omega_m^{-1/2} (1+z)^{-5/2}$.

4 Further collapse

In absence of H₂ cooling the metal-free primordial gas collapses quasi-isothermally. The high Jeans mass ($\sim 10^5 M_{\odot}$) due to the high temperature ($\sim 10^4$ K) inhibits fragmentation and also ensures gas accretion onto the central proto-star at a very high rate, $\dot{M} \sim 1 M_{\odot} \text{ yr}^{-1}$. The result of this could be either of two scenarios, (i) the collapsing gas with a little initial angular momentum turns into a supermassive star (SMS) $M \sim 10^5 M_{\odot}$, or (ii) if the initial angular momentum is high, a rotationally supported massive accretion disk forms around a relatively less massive ($\sim 100 M_{\odot}$) proto-star at the centre. Both the cases result in a massive black hole ($M_{\bullet} \sim 10^5 M_{\odot}$) at the centre within a Myr time scale, which subsequently grows into a

high redshift SMBH. Since simulations indicate the Peeble’s parameter $\lambda \sim 0.07$, it is likely that the final collapse occurs through a supermassive disk phase in most cases without a supermassive star (see Figure 7).

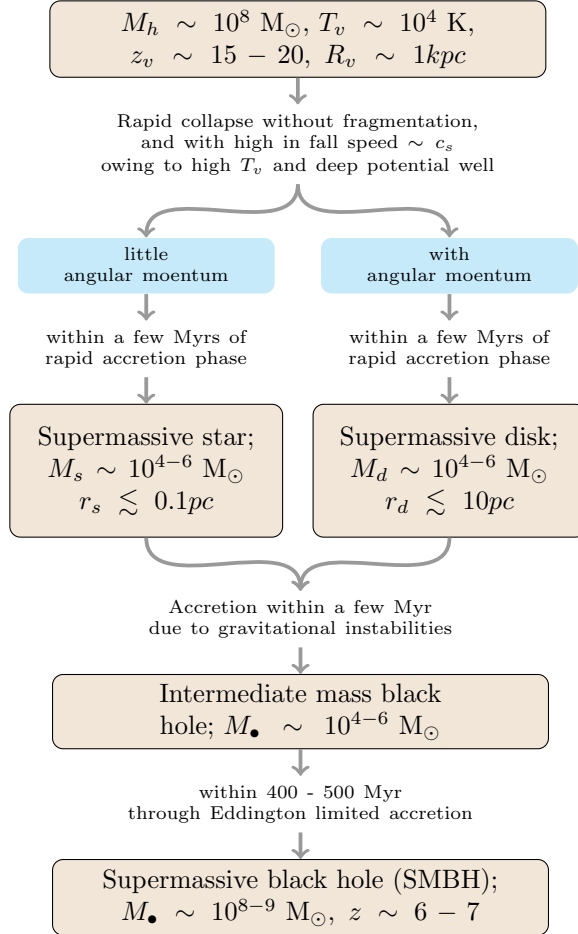


Figure 7: Flowchart of the proposed DCBH model for the formation of SMBH at high redshift

4.1 Angular momentum transfer

The case when a rotationally supported disk forms around a proto-star, the angular momentum transfer has to be very efficient for it to turn into a massive black hole within the stipulated time scale. Previous studies show that the angular momentum transfer due to α -viscosity is very ineffective. The major sources of angular momentum transfer could be the radiative viscosity, radiative drag and gravitational instabilities (Mangalam, 2001, and the references therein). We briefly discuss these two scenarios in the following sections.

4.1.1 CBR drag

Cosmic background radiation (CBR) drag due to Compton friction can play an effective role in removing the angular momentum from a highly ionized ($x \approx 1$) disk at high redshifts (see Figure 8). A self-similar collapse of a highly ionized ($x \approx 1$) Mestel disk due to the Compton drag of CBR is given by [Mangalam (2003); suitably scaled],

$$\xi(z) = \exp \left[-0.4 \times 10^2 \left(\frac{1+z}{1000} \right)^{5/2} \left(1 - \left(\frac{1+z}{1+z_i} \right)^{5/2} \right) \right] \quad (33)$$

where z_i is the redshift of the formation of the (ionized) disk. We see that the CBR drag is very effective at high redshifts and can give rise to huge collapse at high redshifts, but if the disk is formed at low redshifts

($z \lesssim 200$) then the CBR drag may not play any important role in collapsing the disk due to inefficient angular momentum transfer (Figure 9).

For the CBR drag to work as an efficient mechanism for angular momentum transfer, the collapse redshift of the dark matter halo should be very high $\gtrsim 400$. At these redshifts, in a scenario with $M_h \sim 10^{4-5} M_\odot$, it may be statistically possible in low spin systems with efficient cooling without fragmentation to produce a supermassive disk which can collapse by CBR drag (Mangalam, 2003).

4.1.2 Gravitational instabilities

Once a supermassive disk forms, gravitational instabilities can be effective means of angular momentum transport for the further collapse in the DCBH scenario occurring at $z = 9 - 15$. A rotating disk can become unstable under its own gravity as soon as the Toomre parameter goes less than 1 (Toomre, 1964),

$$Q = \frac{c_s \omega}{\pi G \Sigma} < 1 \quad (34)$$

where c_s is the sound speed, ω is the rotation speed and Σ is the surface density of the disk, and G is the gravitational constant. The corresponding time scale of formation of a central massive black hole can be written as (Mangalam, 2001),

$$\begin{aligned} t_g &= \frac{\omega M}{2\pi \Pi_{r\phi}^g} \\ &= 4 \text{ Myr} \cdot \mathcal{M}_{10}^{1/2} \left(\frac{15}{1+z_c} \right) \left(\frac{0.1}{f_b} \right) \left(\frac{0.1}{\alpha_g} \right) m_{\bullet 8} \end{aligned} \quad (35)$$

where \mathcal{M}_{10} is the mass of the halo in units of $10^{10} M_\odot$, $\Pi_{r\phi}^g$ is the viscous stress due to gravitational instabilities, z_c is the redshift of collapse (formation of the disk), $m_{\bullet 8}$ is the black hole mass in units of $10^8 M_\odot$ and $f_b = \Omega_b / \Omega_m$.

Such collapse time scales are applicable for black hole formation via supermassive disks even with some initial angular momentum, by $z \sim 7$, which may be obtained through the process of DCBH described above. Further detailed investigation of the physics and demographics of such black holes will be presented in a future work.

5 Conclusions

We use the most recent bound on the accreting primordial black holes, and adopt a simple model for the heating produced by these accreting primordial black holes, and we find that the accreting primordial black holes of masses $\gtrsim 10^{-2} M_\odot$ could be a potential source of heating in a direct collapse black hole scenario.

We take a simple approach to quantify the effect of possible primordial black holes comprising a fraction of dark matter, on the DCBH scenario of the formation of super massive black holes. We take reasonable mass-accretion rates and the radiative efficiency of the accretion, but at the same time, we have taken caution to make our calculation as conservative as possible so that we do not over estimate the effect. Also, we have used a simple model for the dynamical collapse of the gas. Nonetheless, our calculation shows that possible accreting primordial black holes of masses around $\lesssim 10 M_\odot$ could be another potential source of heating in the context of the thermodynamical evolution of the galaxies and their central black holes.

Though our model requires a good fraction of dark matter to be made up of primordial black holes, we argue here that this possibility is not yet ruled out by the current observational constraints on primordial black hole abundances. Moreover, the fact that no dark matter particles have been observed by the worlds most sensitive direct-detection experiments till now (Akerib et al., 2017; PandaX-II Collaboration et al., 2017; Aprile et al., 2017), casts a doubt on the particle physics based dark matter models. Though, we have strong constraints on the PBH abundances coming from various observations, most of these constraints are applied to a certain mass window and are based on the assumption that the PBH mass function is monochromatic which is unrealistic. With an extended mass function for the PBH it may be possible to explain all the dark matter, even if the density in any particular mass band is small and within the observational bounds [a more detailed discussion on this topic can be found in Carr et al. (2016, 2017);

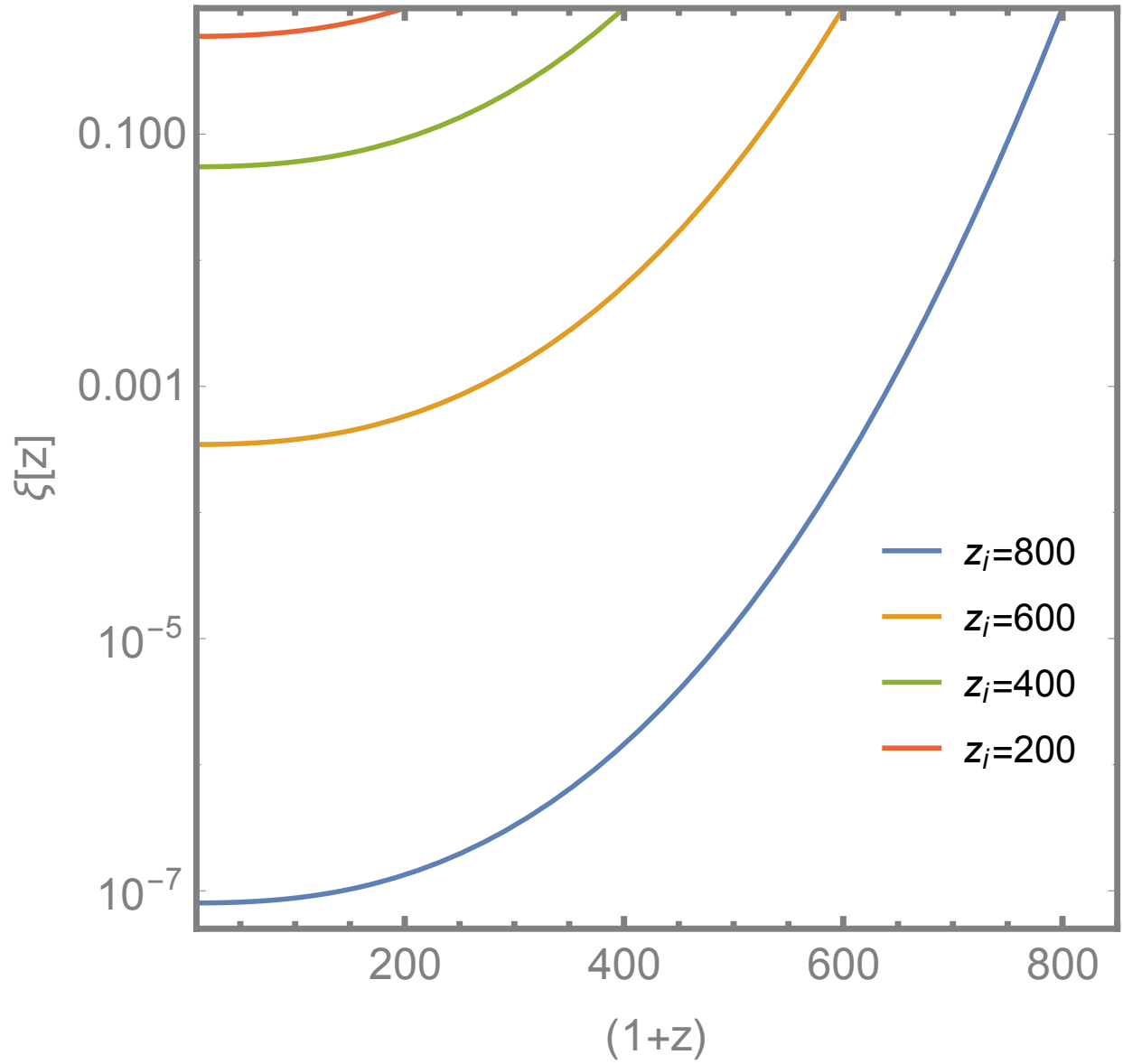


Figure 8: A plot of the collapse factor, $\xi(z) = r(z)/r(z_i)$, due to CBR drag at high redshifts.

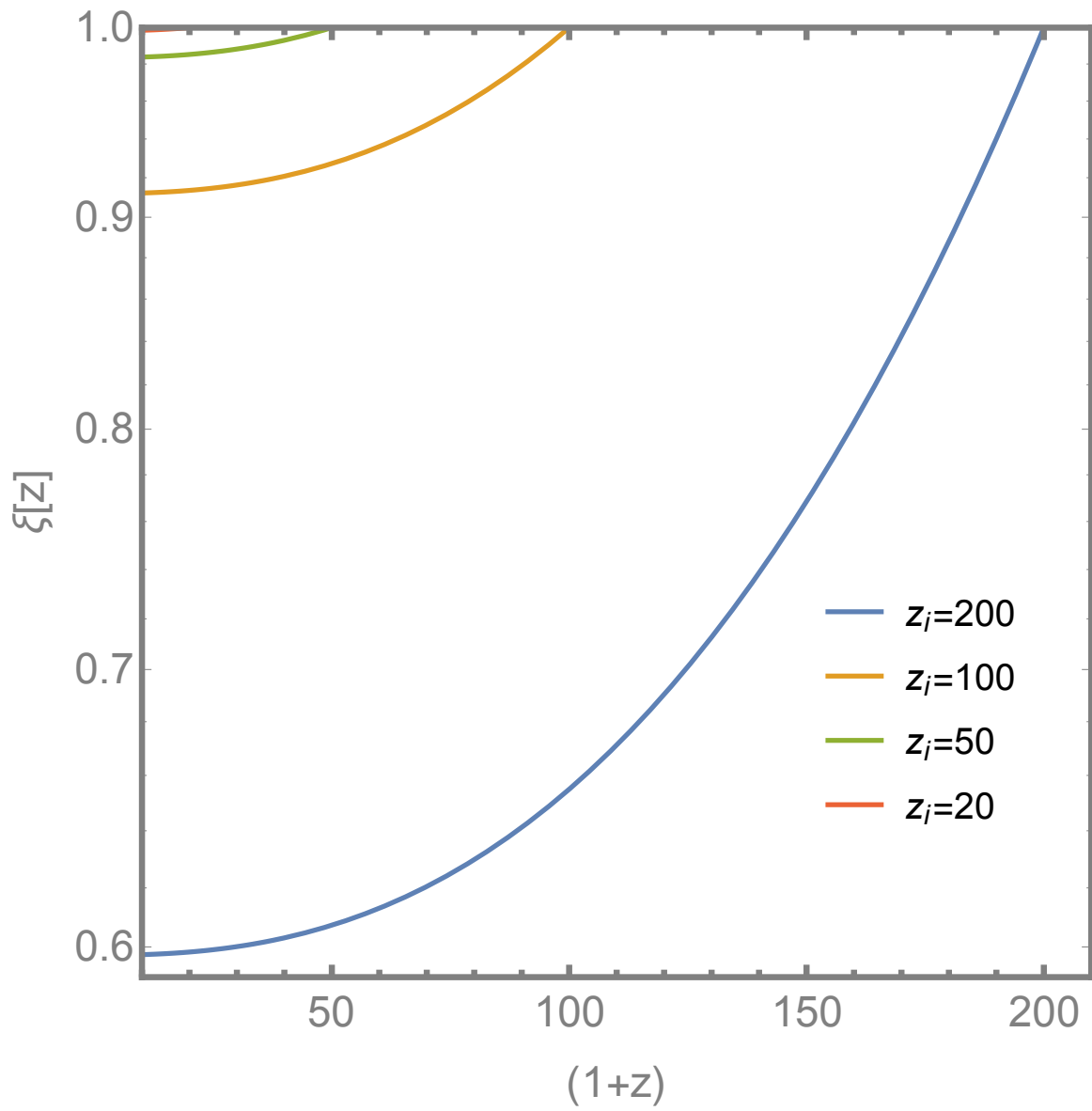


Figure 9: A plot of the collapse factor, $\xi(z) = r(z)/r(z_i)$, due to CBR drag at low redshifts.

[Kühnel & Freese \(2017\)](#)]. Nonetheless, the monochromatic bounds provide a platform to carry out our calculations to make a conservative estimate about the possible effects of primordial black holes during the phase of early structure formation.

Though the current constraints on PBH are not very robust and should be taken as an order of magnitude estimate, the upcoming data from experiments such as the release of final Planck high ℓ data and results from advanced LIGO experiments can play an important role in boosting or ruling out the PBH hypothesis of the dark matter. Also, future and current searches [such as [Gaggero et al. \(2017\)](#)] of possible PBHs around galactic ridge region in the Milky Way using careful measurements of radio and X-ray emission coming from the accretion of gas onto the population of PBHs can be a key to establishing or debunking the PBH hypothesis.

In the future, we plan to carry out a detailed analysis, using a well-motivated extended mass function for the primordial black hole mass distribution, and also incorporating an efficient mechanism of angular momentum transfer in the collapse physics.

Acknowledgement

We thank the referees for useful comments. KLP thanks Shiv Sethi for many useful discussions.

References

- Abel, T., Bryan, G. L., & Norman, M. L. 2002, *Science*, 295, 93
- Akerib, D. S., Alsum, S., Araújo, H. M., et al. 2017, *Physical Review Letters*, 118, 021303
- Ali-Haimoud, Y., & Kamionkowski, M. 2017, *Phys. Rev. D*, 95, 043534
- Aprile, E., Aalbers, J., Agostini, F., et al. 2017, *Physical Review Letters*, 119, 181301
- Begelman, M. C., Volonteri, M., & Rees, M. J. 2006, *MNRAS*, 370, 289
- Bondi, H. 1952, *MNRAS*, 112, 195
- Bovino, S., Schleicher, D. R. G., & Grassi, T. 2014, *A&A*, 561, A13
- Bromm, V., Coppi, P. S., & Larson, R. B. 2002, *ApJ*, 564, 23
- Bromm, V., & Loeb, A. 2003, *ApJ*, 596, 34
- Carr, B., Raidal, M., Tenkanen, T., Vaskonen, V., & Veermäe, H. 2017, *Phys. Rev. D*, 96, 023514
- Carr, B., Kühnel, F., & Sandstad, M. 2016, *Phys. Rev. D*, 94, 083504
- Clark, S. J., Dutta, B., Gao, Y., Strigari, L. E., & Watson, S. 2017, *Phys. Rev. D*, 95, 083006
- Gaggero, D., Bertone, G., Calore, F., et al. 2017, *Physical Review Letters*, 118, 241101
- Galli, D., & Palla, F. 1998, *A&A*, 335, 403
- Haiman, Z. 2004, *ApJ*, 613, 36
- Hawking, S. 1971, *MNRAS*, 152, 75
- Heinz, S., & Sunyaev, R. A. 2003, *MNRAS*, 343, L59
- Hollenbach, D., & McKee, C. F. 1979, *ApJS*, 41, 555
- Kühnel, F., & Freese, K. 2017, *Phys. Rev. D*, 95, 083508
- Madhavacheril, M. S., Sehgal, N., & Slatyer, T. R. 2014, *Phys. Rev. D*, 89, 103508
- Mangalam, A. 2003, *Bulletin of the Astronomical Society of India*, 31, 207
- Mangalam, A. 2001, *A&A*, 379, 1138
- Mortlock, D. J., Warren, S. J., Venemans, B. P., et al. 2011, *Nature*, 474, 616
- Narayan, R., & Yi, I. 1995, *ApJ*, 452, 710
- Oh, S. P., & Haiman, Z. 2002, *ApJ*, 569, 558
- O’Shea, B. W., & Norman, M. L. 2007, *ApJ*, 654, 66
- Omukai, K. 2001, *ApJ*, 546, 635
- PandaX-II Collaboration, :, Cui, X., et al. 2017, *Physical Review Letters*, 119, 181302
- Park, M.-G., & Ostriker, J. P. 2001, *ApJ*, 549, 100
- Rice, J. R., & Zhang, B. 2017, *Journal of High Energy Astrophysics*, 13, 22
- Ricotti, M., Ostriker, J. P., & Mack, K. J. 2008, *ApJ*, 680, 829-845
- Safronek-Shrader, C., Agarwal, M., Federrath, C., et al. 2012, *MNRAS*, 426, 1159

Salpeter, E. E. 1964, *ApJ*, 140, 796

Sethi, S., Haiman, Z., & Pandey, K. 2010, *ApJ*, 721, 615

Sethi, S. K., Nath, B. B., & Subramanian, K. 2008, *MNRAS*, 387, 1589

Shakura, N. I., & Sunyaev, R. A. 1973, *A&A*, 24, 337

Shang, C., Bryan, G. L., & Haiman, Z. 2010, *MNRAS*, 402, 1249

Smith, A., Bromm, V., & Loeb, A. 2016, *MNRAS*, 460, 3143

Smole, M., Micic, M., & Martinović, N. 2015, *MNRAS*, 451, 1964

Tisserand, P., Le Guillou, L., Afonso, C., et al. 2007, *A&A*, 469, 387

Toomre, A. 1964, *ApJ*, 139, 1217

Trenti, M., & Stiavelli, M. 2009, *ApJ*, 694, 879

Volonteri, M. 2007, *ApJ*, 663, L5

Volonteri, M., & Bellovary, J. 2012, *Reports on Progress in Physics*, 75, 124901

Volonteri, M., & Rees, M. J. 2005, *ApJ*, 633, 624

Wu, X.-B., Wang, F., Fan, X., et al. 2015, *Nature*, 518, 512